Detecting the Elusive P-Wave: A New ECG Lead to Improve the Recording of Atrial Activity

Alan Kennedy*, *Student Member, IEEE*, Dewar D. Finlay, Daniel Guldenring, Raymond R. Bond, and James McLaughlin, *Member, IEEE*

***Abstract*—*Goal:* In this study, we report on a lead selection method that was developed to detect the optimal bipolar electrode placement for recording of the P-wave. *Methods:* The study population consisted of 117 lead body surface potential maps recorded from 229 healthy subjects. The optimal bipolar lead was developed using the training set (172 subjects) then extracted from the testing dataset (57 subjects) and compared to other lead systems previously reported for improved recording of atrial activity. All leads were assessed in terms of P-wave, QRS, and STT root mean square (RMS). The P/QRST RMS ratio was also investigated to determine the atrioventricular RMS ratio. Finally, the effect of minor electrode misplacements on the P-lead was investigated. *Results:* The P-lead discovered in this study outperformed all other investigated leads in terms of P-wave RMS. The P-lead showed a significant improvement in median P-wave RMS (93 versus 72 μV, $p < 0.001$) over the next best lead, Lead II. An improvement in QRS and STT RMS was also observed from the P-lead in comparison to lead II (668 versus 573 μV, $p < 0.001$) and (327 versus 196 μV, $p < 0.001$). Although P-wave RMS was reduced by incorrect electrode placement, significant improvement over Lead II was still evident. *Conclusion:* The P-lead improves P-wave RMS signal strength over all other investigated leads. Also the P-lead does not reduce QRS and STT RMS making it an appropriate choice for atrial arrhythmia monitoring. *Significance:* Given the improvement in signal-to-noise ratio, an improvement in algorithms that rely on P-wave analysis may be achieved.**

***Index Terms*—Biomedical signal processing, electrocardiogram (ECG), P-wave, signal-to-noise ratio (SNR).**

I. Introduction

A fundamental challenge in surface electrocardiogram (ECG) monitoring is to discern small but diagnostically relevant signals, such as P-waves, from background noise. Detection and analysis of the P-wave on the ECG allows for assessment of atrioventricular conduction and, as such, more accurate diagnosis of cardiac arrhythmias, in particular, atrial fibrillation (AF) [1]. Thromboembolic events such as transient ischemic attack and stroke can be attributable to AF [2]. Strokes due to AF are common and can be devastating with approximately 70% to 80% of patients becoming permanently disabled or dying [3]. These events are preventable with appropriate intervention [4]. However, because AF is often sporadic, intermittent (Paroxysmal AF), and asymptomatic, it can be difficult to detect using standard detection methods.

The majority of automated AF detection algorithms rely solely on the analysis of R–R intervals. This can lead to false positives due to the presence of other cardiac conditions such as sinoatrial block, ventricular systole, ectopic beats, and supraventricular tachycardia [5]. An improvement in P-wave detection may lead to improved detection of atrial arrhythmias such as AF, atrial flutter, and atrial tachycardia [6]. This has prompted renewed interest in patient monitoring technology, particularly Holter monitoring systems for 24–72 h continuous ECG monitoring [7].

Where signal information has been considered in lead selection, most ECG lead systems have been optimized for recording of ventricular activity. As a result, it is assumed that an optimized bipolar ECG lead could improve the detection of the P-wave, maximizing signal strength and therefore signal-to-noise ratio (SNR). P-waves traditionally are difficult to record, especially during ambulation. This is mainly due to a low SNR and the fact that P-waves have no exclusive time or frequency characteristics [8].

Often P-waves from standard ECG leads are indiscernible from electrostatic noise as a result of incorrect skin preparation, patient movement, or skeletal muscle potential [9]. Traditionally, Holter monitors often rely on a reduced number of ECG leads (usually 1–3) for long-term continuous ECG monitoring. Single-lead ECG systems have a higher patient acceptability when compared to 12-lead and 3-lead monitors due to the reduced number of electrodes and wires [10]. However, this improvement in patient acceptability comes at a cost of a significant reduction in the ECG information captured. In this study, we determine the recording sites for a bipolar lead that is optimized for the recording of atrial activity during normal atrial activation.

II. Background

A. Body Surface Potential Maps (BSPMs)

In comparison to all other recording formats, BSPMs provide the best indication of the spatial distribution of electrical potentials on the thorax. However, BSPMs are difficult to record in a clinical setting. As a result, the standard 12-lead has not been surpassed as the clinical standard for the detection of cardiac arrhythmias [11].

Manuscript received February 26, 2015; revised May 25, 2015; accepted June 16, 2015. Date of publication June 26, 2015; date of current version January 16, 2016. This work was supported by The Northern Ireland Connected Health Innovation Centre and by the Department for Employment and Learning, Northern Ireland. *Asterisk indicates corresponding author.*

*A. Kennedy is with the Nanotechnology and Integrated BioEngineering Centre, University of Ulster, Northern Ireland BT37 0QB, U.K. (e-mail: kennedy-a23@email.ulster.ac.uk).

D. D. Finlay, D. Guldenring, R. R. Bond, and J. McLaughlin are with the University of Ulster.

Color versions of one or more of the figures in this paper are available online at http://ieeexplore.ieee.org.

Digital Object Identifier 10.1109/TBME.2015.2450212

B. Standard 12-Lead ECG

The electrode positions for recording of the 12-lead ECG are suboptimal in capturing atrial activity. Previous studies have shown that Lead II and precordial Lead V1 provide the most P-wave signal strength [12]. Lux and Greg [1] demonstrated that Leads II, III, and V1 provided the greatest P-wave signal strength in comparison to all other leads of the standard 12-lead ECG. Optimization of the standard 12-lead ECG for atrial activity has also previously been investigated [13]. This optimized system, referred to as the atrialcardiogram (ACG), used the same number of electrodes as the 12-lead ECG however the precordial leads were repositioned in closer proximity to the right atrium and left atrium.

C. Modified Lead Systems for Recording Atrial Activity

In 1910, Sir T. Lewis became the first to implement an optimized bipolar ECG lead for improved recording of atrial activity. During his pioneering work in AF, Lewis discovered that placing electrodes at the right forth-intercostal space and the right second-costochondral junction increased the amplitude of atrial activity [14].

This ECG lead would later go on to be named the Lewis lead. The Lewis lead has been shown to increase P-wave amplitude during wide-QRS tachycardia [15]. However, a comprehensive study by Madias [16] demonstrated that P-wave amplitude from the Lewis lead is not greater than the best lead of the 12-lead ECG in patients with a range of cardiac illnesses. The Barker lead [17] often referred to as the vertical sternal lead or ES on the EASI lead system [18], involves placement of electrodes at the xiphoid process and below the suprasternal notch of the manubrium. Herzog *et al.* [19] demonstrated that the Barker lead recorded greater P-wave signal than that of the standard ECG leads and the Lewis lead.

Nedios *et al.* [20] reported that the best performing electrode positions for a bipolar lead for P-wave amplitude was approximately the second right intercostal space and 1 in above the xiphoid process inline with the fourth intercostal space.

More recently, a study by Pentrénas *et al.* [6] suggested a modified version of the Lewis Lead for the ambulatory monitoring of atrial arrhythmias. They moved the first electrode to superior sternum and the second electrode from the fourth intercostal space to the fifth intercostal in an effort to reduce motion artifact from arm movement. Results showed that the P-wave amplitude from this modified Lewis Lead was three times greater than the original Lewis Lead. All lead systems investigated in this study are shown in Fig. 1.

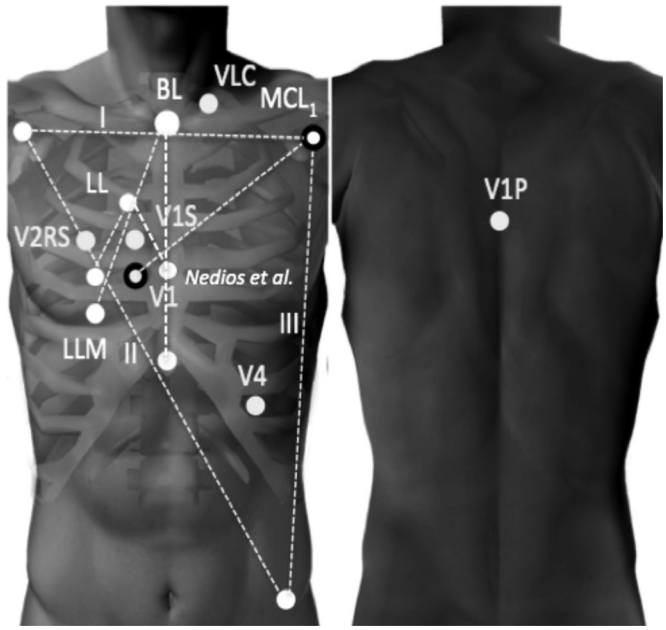

Fig. 1. Modified bipolar and unipolar ECG leads for improved recording of atrial activity.

III. Study Population

The study population consisted of 117-lead BSPMs from 229 healthy subjects. The procedure for recording the data and the data itself have previously been described in [21], [22]. ECG recordings at the 117 recording sites were sampled with respect to Wilson's central terminal resulting in 117 unipolar ECG leads. Each ECG lead was sampled simultaneously for 15 s at a frequency of 500 Hz with a sampling resolution of 10 μV. The information from each ECG lead was reduced using selective linear averaging of the P-wave, QRS complex, and STT segment individually resulting in a single PQRST complex. All measurements of ECG time integrals were then made from superimposed Frank X, Y, and Z leads. In order to provide greater spatial resolution, the 117-lead BSPMs were transformed using a Laplacian 3-D interpolation procedure into 352 nodes which correspond to the nodes on the Dalhousie torso [23]. Some of the required electrocardiographic leads were not available as a direct subset of the interpolated BSPMs. Further electrode positions were then obtained using linear interpolation. This method of interpolation has been reported to produce interpolation errors that are smaller than the level of noise typically found in the precordial leads [24]. The data were then split into a training set consisting of 172 patients and a testing set consisting of the remaining 57 subjects.

IV. Method

A. ECG Processing and Data analysis

For this study, we implemented a method of determining the point in time where the maximum P-wave amplitude occurs across all 352 nodes for each subject. The method is outlined as

$$P_{\mathrm{diff}}(n) = P_{\max}(n) - P_{\min}(n) \tag{1}$$

where $P_{\mathrm{diff}}(n)$ is the maximal P-wave amplitude for a defined point in time *n*, $P_{\max}$ is the maximum P-wave value across all 352 BSPM nodes at *n*, $P_{\min}$ is the minimum P-wave value across all 352 BSPM nodes at *n*.

The point in time containing the maximum P-wave amplitude for each subject was defined as the instance in time where the greatest differential P-wave (Fig. 2) occurred.

TABLE I
ELECTRODE POSITIONS FOR STANDARD AND MODIFIED LEADS FOR IMPROVED RECORDING OF ATRIAL ACTIVITY

Bipolar Leads		
Lead	Negative Electrode	Positive Electrode
I	Right shoulder	Left shoulder
II	Right shoulder	Left hip
III	Left Shoulder	Left hip
Lewis	Second right costochondral junction.	Fourth right intercostal space 1″ right of sternum
Modified Lewis	Superior Sternum	Fifth right intercostal space 1″ right of sternum
ES	Superior Sternum	Xiphoid Process
MCL_1	Left Shoulder	Fourth right intercostal space at the sternal border
Nedios *et al.*	Second right intercostal space	1″ above the xiphoid process inline with the 4th intercostal space.

Unipolar Leads	
Lead	Electrode Position
V1	Fourth right intercostal space at the right sternal border
V2	Fourth right intercostal space at the left sternal border
V3	Midway between V2 and V4
V4	Fifth intercostal space in mid-clavicular line
V5	Left anterior axillary line at same horizontal level as V4
V6	Left mid-anxillary line at same horizontal level as V4 and V5
V1 S	Third right intercostal space at the sternal border
V2 RS	Third right intercostal space at the mid-clavicular line
VLC	Above the left sternoclavicular junction
V1 P	Fourth right intercostal space at the sternal border on the back

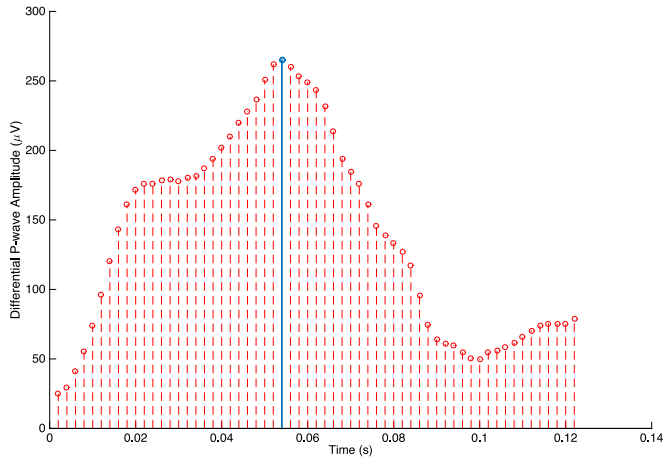

Fig. 2. Differential P-wave values for one subject. The maximum difference in P-wave amplitude across all 352 nodes occurred at 0.054 s (solid line).

P-wave values at this point in time were then extracted across all 352 nodes. Each subjects P-wave value were normalized between 0 and 1, as outlined in (2). This step was taken to alleviate the bias attributable to dominant p-wave values from individual subjects

$$P_{\text{norm}} = \frac{P_{\text{amp}} - \min(P_{\text{amp}})}{\max(P_{\text{amp}}) - \min(P_{\text{amp}})} \tag{2}$$

where P_{norm} is the normalized P-wave values and P_{amp} is the nonnormalized P-wave values. This method was repeated for all 172 subjects of the training set producing one BSPM, of P-wave amplitudes, for each subject. A population based P-wave BSPM was then calculated by taking the median of the P-wave potentials on each node of the BSPM across all 172 subjects, resulting in a single BSPM of P-wave amplitudes across the population. From this median BSPM, the population-based optimal bipolar lead was defined as the location of the maximum and minimum P-wave amplitude.

B. Lead Evaluation

The performance of the population-based optimal bipolar lead was assessed in terms of signal strength and compared to the lead systems described in Table I. Each lead system was also assessed in terms of QRS and STT signal strength in order to determine if any QRS or STT signal strength had been lost when optimizing the bipolar electrode placement for the P-wave. This assessment allows for the identification of the ECG lead with the best signal strength for both the P-wave and the QRS. Previous work has shown that, for accurate detection of atrial arrhythmias such as AF, a combination of both R–R interval and P-wave analysis is advantageous [25]. This, therefore, requires both the QRS complex and the P-wave to have high SNRs.

1) Signal Strength: Experiments were conducted to compare signal root-mean-square (RMS) and signal amplitude of the P-wave, QRS complex, and STT segment from the optimized ECG lead to that which would be obtained from the standard and previously reported lead systems described in Table I.

2) Atrioventricular Ratio: Many P-wave detection algorithms rely on QRST cancellation through template subtraction [26] or wavelet decomposition [27]. When selecting leads for QRST cancellation methods Lead II and V1 are often chosen due to an increased atrioventricular ratio [12]. In this study, all investigated leads were assessed in terms of P/QRST RMS ratio to identify which lead is the most appropriate for QRST cancellation.

3) Electrode Misplacement: ECG electrode misplacement is a common error encountered in clinical practice with up to 36% of 12-lead ECGs recorded using incorrect electrode positions [28]. ECG signal strength and morphology can differ greatly due

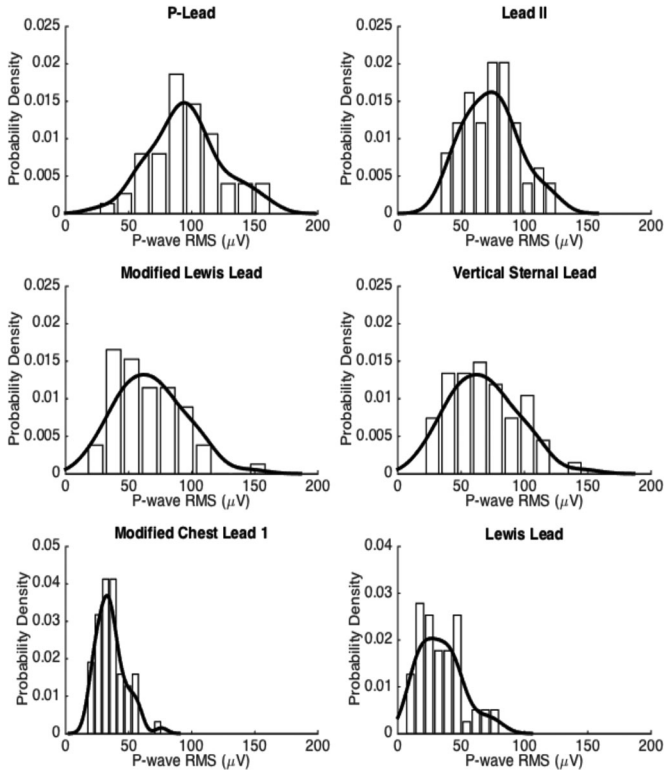

Fig. 3. Density distribution of six leads included in the study.

to incorrect electrode placement. Previous studies have shown that when applying the precordial leads of the 12-lead ECG an average electrode misplacement of 1.14 in is observed [29]. This can lead to false positives and false negatives when monitoring for arrhythmias. In this study, we investigated the effects of electrode misplacement on P-wave signal strength from the P-lead.

The electrodes were repositioned to four incorrect locations in a 0.5-in radius around the correct electrode locations shown in Fig. 4. This resulted in 16 potential misplacement scenarios. Median P-wave RMS and the interquartile range were then calculated to allow for a comparison between scenarios.

C. Statistical Analysis

The primary analysis compared P-wave RMS values from the best performing lead (P-lead) to the second best performing lead (lead II). As the results are not normally distributed (see Fig. 3), the median value of the signal RMS and interquartile range was calculated for each lead across all 57 subjects in the test data in order to provide a measure of performance. A comparison of the median RMS values between the different leads was then performed using the Wilcoxon signed-rank test [30].

V. Results

The maximum attainable P-wave RMS signal strength for the lead configurations under investigation are provided in Table II. The P-lead outperformed the other lead systems under investigation. The median P-wave RMS from the P-lead was significantly (Wilcoxon signed-rank test, $\alpha = 0.05$) greater than

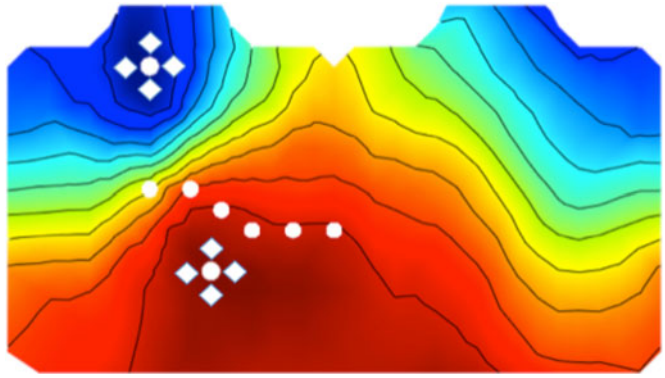

Fig. 4. Median BSPM of normalized P-wave amplitude from the 172 subjects of the training dataset, including the P-lead electrode placement and the location of the precordial leads. The P-lead is recorded between node 43 and node 255 on the Dalhousie torso [23]. The electrode positions used to simulate electrode misplacement (♦) are placed around the original P-lead electrode positions (O) in white.

from the next best lead, Lead II, (93 versus 72 μV, $p < 0.001$). Median P-wave amplitude recorded from the P-lead was also improved (164 versus 132 μV, $p < 0.001$). The findings of the experiments investigating signal RMS and signal amplitude for the P-wave, QRS complex, and STT segment across all lead systems under investigation can be seen in Table II (see also Table III and Figs. 5 and 6). The P-lead captured the greatest P-wave RMS without reducing QRS or STT signal strength. Anatomical locations of the bipolar P-lead electrodes are shown in Fig. 7.

VI. Discussion

Historically P-waves have been difficult to detect, possibly due to the fact that many lead systems focus primarily on the optimal detection of ventricular events. The ventricles differ greatly from the atrium in terms of spatial location, orientation, and signal amplitude [31]. Recording of atrial activity is therefore not optimal from many lead systems and a lead system for the recording of atrial activity is highly desirable. In the previous sections, we have outlined a method that results in a bipolar ECG lead that allows for maximum P-wave signal strength. This method was designed to account for the known variance in P-wave morphology across ECG leads [32]. The method described uses are based upon a simple analysis of the atrial information in each BSPM, determining the point in time where the greatest difference in P-wave amplitude occurred. The optimized lead found in this study demonstrated a significant improvement in median P-wave RMS (93 versus 72 μV, $p < 0.001$) and median P-wave amplitude (164 versus 132 μV, $p < 0.001$) over the next best lead, lead II. An improvement in median QRS signal strength (668 versus 573 μV, $p < 0.001$) and median QRS amplitude (1660 versus 1472 μV, $p < 0.001$) was also observed. The findings demonstrate the effectiveness of the P-lead in capturing maximum information during atrial depolarization without compromising QRS signal strength. The P-lead could be used in applications such as long-term ambulatory ECG monitoring for atrial arrhythmias, which requires maximum SNR during both atrial and ventricular depolarization.

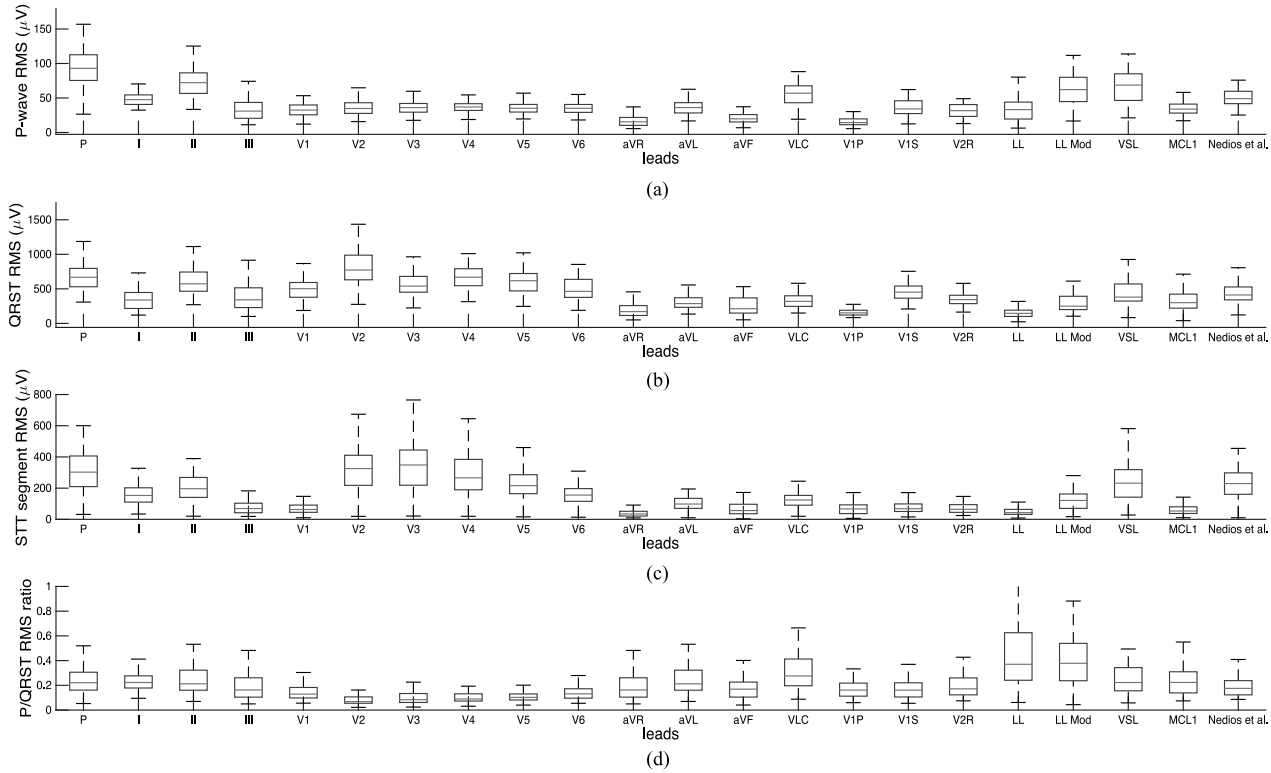

Fig. 5. Performance of the P-lead in comparison with standard and modified lead systems. For (a) P-wave RMS (b) QRS RMS. (c) STT segment RMS and (d) P/QRST ratio. Based on median values the P-lead improves both P-wave RMS (93 versus 72 μV, $p < 0.001$), QRS RMS (668 versus 573 μV, $p < 0.001$), and STT segment RMS (303 versus 196 μV, $p < 0.001$) over lead II.

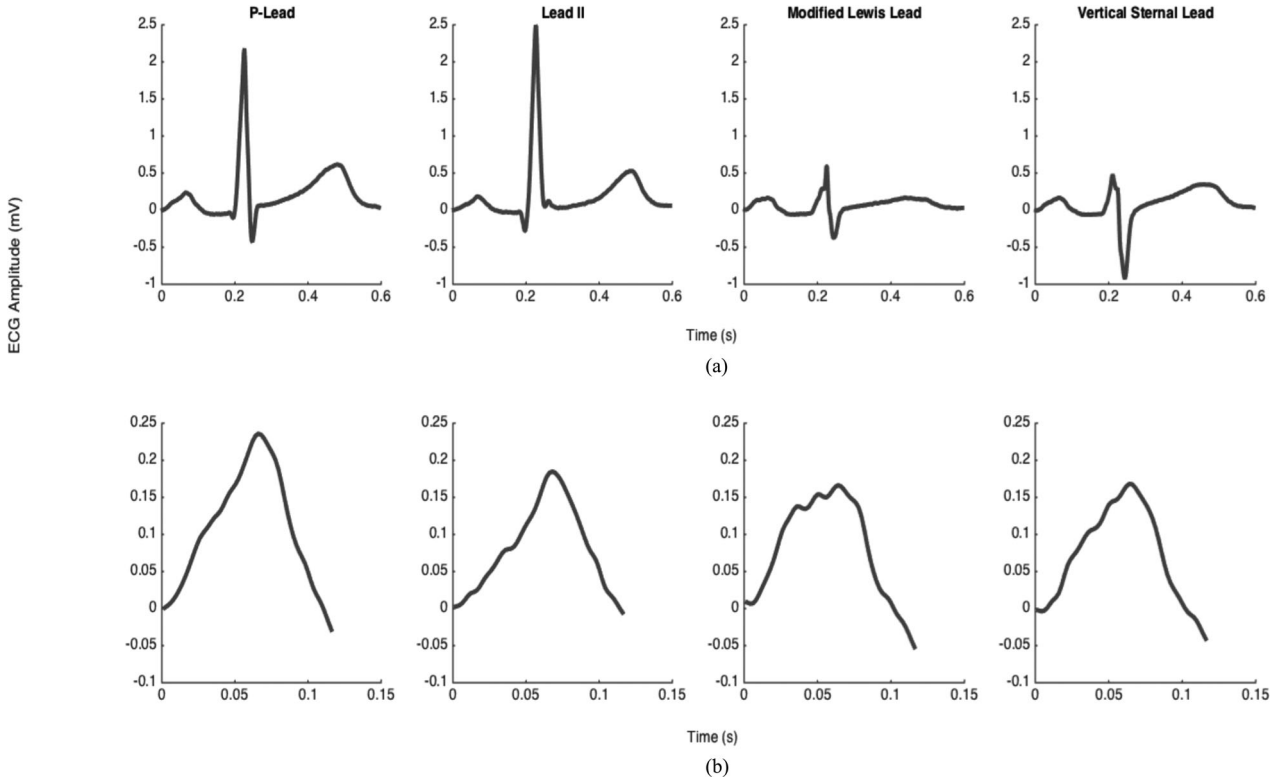

Fig. 6. Example of (a) One ECG beat and (b) P-wave from the four best performing leads in terms of P-wave RMS. It can be seen that although the P-lead does provide the best P-wave signal strength, the modified Lewis and vertical sternal leads provide an improved P/QRST RMS ratio.

TABLE II
PERFORMANCE OF LEADS IN CAPTURING P-WAVE, QRS COMPLEXES, AND STT SEGMENTS

Lead	P-Wave RMS (μV)	P-Wave Amplitude (μV)	QRS RMS (μV)	QRS Amplitude (μV)	STT RMS (μV)	STT Amplitude (μV)	P/QRST RMS Ratio
P	93 (75;113)	164 (133;188)	668 (526;807)	1660 (1276;2008)	303 (208;408)	601 (422;780)	0.22 (0.16;0.31)
I	48 (41;55)	13 (3;21)	338 (212;453)	187 (87;274)	153 (107;204)	11 (5;23)	0.22 (0.18;0.28)
II	72 (56;87)	132 (98;153)	573 (460;744)	1472 (1149;1843)	196 (140;269)	401 (294;552)	0.21 (0.16;0.32)
III	31 (21;44)	54 (37;84)	341 (228;522)	876 (434;1419)	69 (42;104)	118 (39;216)	0.16 (0.10;0.27)
V1	32 (25;40)	49 (38;61)	503 (374;593)	294 (157;439)	63 (45;91)	76 (41;140)	0.13 (0.10;0.18)
V2	35 (27;43)	69 (44;86)	773 (625;995)	630 (412;851)	325 (215;412)	599 (338;781)	0.07 (0.05;0.11)
V3	36 (29;42)	67 (50;84)	540 (450;681)	877 (637;1224)	349 (217;452)	643 (403;815)	0.08 (0.06;0.13)
V4	37 (32;42)	67 (57;78)	669 (542;799)	1580 (1246;2000)	266 (189;385)	514 (348;746)	0.09 (0.07;0.13)
V5	35 (29;41)	62 (51;73)	618 (470;727)	1561 (1197;1842)	216 (164;288)	409 (330;580)	0.10 (0.08;0.13)
V6	35 (29;41)	62 (49;73)	464 (375;639)	1149 (926;1523)	155 (116;199)	313 (241;416)	0.13 (0.10;0.17)
aVL	15 (10;22)	9 (3;14)	171 (114;261)	102 (65;175)	35 (21;52)	12 (6;31)	0.16 (0.10;0.27)
aVR	36 (28;43)	8 (2;12)	287 (230;372)	100 (55;148)	98 (70;134)	11 (5;17)	0.21 (0.16;0.32)
aVF	20 (15;26)	16 (11;27)	213 (149;370)	339 (173;665)	56 (36;100)	21 (11;37)	0.17 (0.10;0.23)
V1C	57 (43;68)	10 (3;18)	319 (246;406)	138 (67;194)	124 (91;154)	12 (6;24)	0.28 (0.20;0.42)
V1P	14 (11;20)	12 (3;20)	152 (121;192)	185 (97;261)	67 (36;94)	12 (4;19)	0.16 (0.11;0.22)
V1S	34 (27;46)	25 (12;39)	453 (365;543)	270 (151;393)	68 (50;100)	51 (27;99)	0.16 (0.11;0.22)
V2R	32 (23;40)	16 (6;24)	344 (285;407)	179 (85;252)	64 (44;96)	29 (15;44)	0.17 (0.12;0.26)
LL	33 (19;44)	59 (35;82)	146 (100;195)	286 (168;445)	43 (31;64)	87 (61;130)	0.37 (0.24;0.63)
LLM	62 (45;80)	109 (87;136)	250 (200;399)	367 (208;636)	121 (70;163)	212 (133;312)	0.38 (0.23;0.54)
VSL	69 (46;85)	121 (87;154)	381 (321;578)	503 (373;823)	232 (142;319)	448 (270;570)	0.22 (0.15;0.35)
MCL1	34 (28;41)	34 (19;52)	300 (219;424)	652 (439;891)	53 (37;81)	44 (18;98)	0.22 (0.14;0.31)
Nedios et al.	49 (42;60)	90 (73;113)	412 (340;528)	395 (265;566)	229 (159;299)	414 (289;573)	0.18 (0.12;0.24)

Values represent median (25th Percentile; 75th Percentile).

TABLE III
PERFORMANCE OF THE P-LEAD DURING 0.5 IN ELECTRODE MISPLACEMENTS

	Positive Electrode	Negative Electrode	P-Wave RMS (μV)
Scenario 1	To the left	Upward	90 (73;109)
Scenario 2	Upward	Upward	92 (77;110)
Scenario 3	To the right	Upward	90 (75;110)
Scenario 4	Downward	Upward	89 (73;110)
Scenario 5	To the left	Left	88 (73;110)
Scenario 6	Upward	Left	92 (76;110)
Scenario 7	To the right	Left	89 (74;110)
Scenario 8	Downward	Left	86 (74;110)
Scenario 9	To the left	Downward	79 (68;113)
Scenario 10	Upward	Downward	84 (71;109)
Scenario 11	To the right	Downward	83 (70;109)
Scenario 12	Downward	Downward	79 (68;113)
Scenario 13	To the left	Right	89 (67;110)
Scenario 14	Upward	Right	91 (72;113)
Scenario 15	To the right	Right	90 (72;111)
Scenario 16	Downward	Right	89 (68;111)

Values represent median and (25th percentile; 75th percentile).

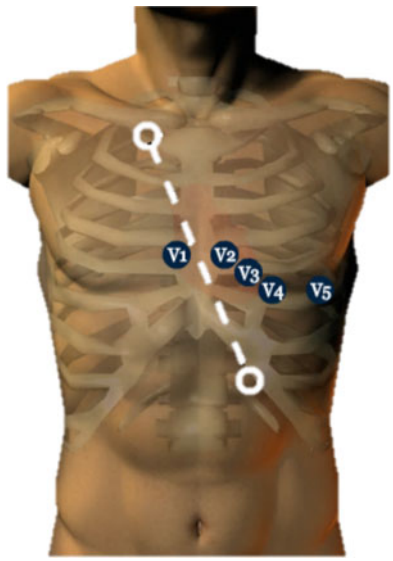

Fig. 7. Optimized electrode placement for maximum P-wave signal illustrated on a human torso schematic. The electrode positions correspond to the right sternal clavicular junction and the midpoint of the left costal margin inline with the seventh intercostal space.

The increased SNR from this bipolar lead may be beneficial to ECG algorithms that rely on P-wave analysis.

Most Holter monitoring systems implement the Mason–Likar leads [33] (I, II, and III) in combination with a single precordial lead for long-term monitoring [34]. More recently, single-lead ECG monitors have been shown to have greater patient acceptability. P-wave signal strength from the P-lead is increased when compared to other lead systems commonly used in arrhythmia monitoring making it an appropriate choice when monitoring for atrial arrhythmias.

It has been shown previously that the most effective AF algorithms incorporate both R–R interval and P-wave analysis [25]. Many algorithms, due to the low SNR (in particular during ambulation), do not utilize P-wave information. The P-lead may allow a different approach to algorithm development in this area and although improved signal strength does not guarantee better algorithm performance improvement is highly likely. The maximum atrial-ventricular RMS ratio was achieved when using the modified Lewis lead. This makes the modified Lewis lead the most appropriate lead for QRST cancellation techniques. This lead, therefore, cannot be used to assess ventricular activity given the reduction in QRS and STT signal strength. Misplacement of the bipolar electrodes used to record the P-lead did cause a significant (Wilcoxon signed-rank test, $\alpha = 0.05$) reduction in

P-wave RMS (93 versus 79 μV, $p<0.001$); however, even with this reduction, the P-lead still significantly (Wilcoxon signed-rank test, $\alpha = 0.05$) outperformed the next best lead, lead II (79 versus 72 μV, $p<0.001$). This demonstrates a robustness of the P-lead to electrode misplacement, which may improve its effectiveness when implemented clinically.

VII. Conclusion

The optimized lead discovered in this research outperformed all other lead systems under investigation in terms of P-wave RMS. What remains to be tested is the performance of automated algorithms using the P-lead. It will be of interest to assess if the improvement in previously described algorithms can be achieved using the P-lead, given the associated improvement in SNR.

The close proximity of the identified electrode positions to the right clavicle and the costal margin are expected to allow accurate electrode positioning in a clinical setting. However, even with small misplacements of the bipolar electrodes (<0.5 inch) a significant improvement in P-wave signal strength over all other leads is still achieved. The electrode positions discovered in this study may also provide better performance in terms of SNR during ambulation due to their central location of the electrode positions on the torso, away from moving body parts and large muscle groups. This study has shown that during normal atrial activation, optimized lead selection can lead to an improvement in P-wave signal strength.

VIII. Future Work

If algorithm improvement is discovered from the improved SNR from the P-lead, an estimation of this lead from standard 12-lead ECGs may prove to be of benefit, particularly in patients with low P-wave amplitude. This will improve P-wave information without changing the standard clinical practice of ECG acquisition. Further investigations must also be performed on patients with atrial arrhythmias to assess if abnormal atrial activation can affect the performance of the P-lead. If so, this would suggest that a two lead system capable of maximizing SNR during both normal and abnormal atrial activation may prove most effective in detecting atrial arrhythmias.

References

[1] R. L. Lux and R. Greg, "New leads for P wave detection and arrhythmia classification," *J. Electrocardiol.*, vol. 37, p. 80, Oct. 2004

[2] J. S. Healey *et al.*, "Subclinical atrial fibrillation and the risk of stroke," *N. Engl. J. Med.*, vol. 366, pp. 120–129, Jan. 2012.

[3] G. Saposnik *et al.*, "Atrial fibrillation in ischemic stroke: Predicting response to thrombolysis and clinical outcomes," *Stroke*, vol. 44, pp. 99–104, Jan. 2013.

[4] R. G. Hart *et al.*, "Meta-analysis: Antithrombotic therapy to prevent stroke in patients who have nonvalvular atrial fibrillation," *Annu. Int. Med.*, vol. 146, pp. 857–867, Jun. 2007.

[5] A. Muller *et al.*, "Reliability of an external loop recorder for automatic recognition and transtelephonic ECG transmission of atrial fibrillation," *J. Telemed. Telecare*, vol. 15, pp. 391–396, Dec. 2009.

[6] A. Petrènas *et al.*, "Modified lewis ECG lead system for ambulatory monitoring of atrial arrhythmias," *J. Electrocardiol.*, vol. 48, pp. 157–163, Mar. 2015.

[7] K. Harris *et al.*, "How can we best detect atrial fibrillation?" *J. Roy. College Physicians Edinburgh*, vol. 42, Suppl 18, pp. 5–22, Mar. 2012.

[8] F. Portet, "P wave detector with PP rhythm tracking: Evaluation in different arrhythmia contexts," *Physiol. Meas.*, vol. 29, p. 141, Jan. 2008.

[9] J. E. Waktare *et al.*, "Optimum lead positioning for recording bipolar atrial electrocardiograms during sinus rhythm and atrial fibrillation," *Clin. Cardiol.*, vol. 21, pp. 825–830, Nov. 1998.

[10] N. Donnelly *et al.*, "Development of a ubiquitous clinical monitoring solution to improve patient safety and outcomes," in *Proc. Conf. IEEE Eng. Med. Biol. Soc.*, 2012, pp. 6068–6073.

[11] M. P. Donnelly *et al.*, "Lead selection: Old and new methods for locating the most electrocardiogram information," *J. Electrocardiol.*, vol. 41, pp. 257–263, May 2008.

[12] L. Mainardi *et al.*, *Understanding Atrial Fibrillation: The Signal Processing Contribution.* San Rafael, CA, USA: Morgan & Claypool Publishers, 2008.

[13] Z. Ihara *et al.*, "Adaptation of the standard 12-lead electrocardiogram system dedicated to the analysis of atrial fibrillation," *J. Electrocardiol.*, vol. 40, pp. 68e1–68e8 Jan. 2007.

[14] M. J. Goldman, *Principles of Clinical Electrocardiography.* Los Altos, CA, USA: Lange Medical Publications, 1956.

[15] W. R. D. Holanda-Miranda *et al.*, "Lewis lead enhances atrial activity detection in wide QRS tachycardia," *J. Emerg. Med.*, vol. 43, pp. 97–99, Aug. 2012.

[16] J. E. Madias, "Comparison of P waves recorded on the standard electrocardiogram, the "Lewis lead" and "saline-filled central venous catheter"—based intracardiac electrocardiogram," *Amer. J. Cardiol.*, vol. 94, pp. 474–478, Aug. 2014.

[17] P. S. Barker *et al.*, "Auricular paroxysmal tachycardia with auriculoventricular block," *Amer. Heart J.*, vol. 25, pp. 765–798, Jun. 1943.

[18] G. E. Dower *et al.*, "Deriving the 12-lead electrocardiogram from four (EASI) electrodes," *J. Electrocardiol.*, vol. 21, pp. S182–S187, 1988.

[19] L. R. Herzog *et al.*, "Evaluation of electrocardiographic leads for detection of atrial activity (P Wave) in ambulatory EGG monitoring: A pilot study," *Pacing Clin. Electrophysiol.*, vol. 15, pp. 131–134, Feb. 1992.

[20] S. Nedios *et al.*, "Precordial electrode placement for optimal ECG monitoring: Implications for ambulatory monitor devices and event recorders," *J. Electrocardiol.*, vol. 47, pp. 669–676, Sep. 2014.

[21] F. Kornreich *et al.*, "Identification of first acute Q wave and non-Q wave myocardial infarction by multivariate analysis of body surface potential maps," *Circulation*, vol. 84, pp. 2442–2453, Dec. 1991.

[22] F. Kornreich *et al.*, "Map representation and diagnostic performance of the standard 12-lead ECG," *J. Electrocardiol.*, vol. 28, pp. 121–123, Jan. 1995.

[23] B. Milan Horácek and J. C. Clements, "The inverse problem of electrocardiography: A solution in terms of single-and double-layer sources on the epicardial surface," *Math. Biosci.*, vol. 144, pp. 119–154, Sept. 1997.

[24] B. J. Schijvenaars *et al.*, "Interpolation of body surface potential maps," *J. Electrocardiol.*, vol. 28, pp. 104–109, Jan. 1995.

[25] S. Babaeizadeh *et al.*, "Improvements in atrial fibrillation detection for real-time monitoring," *J. Electrocardiol.*, vol. 42, pp. 522–526, Nov. 2009.

[26] J. Slocum *et al.*, "Computer detection of atrioventricular dissociation from surface electrocardiograms during wide QRS complex tachycardias," *Circulation*, vol. 72, pp. 1028–1036, Nov. 1985.

[27] L. Senhadji *et al.*, "Wavelets extrema representation for QRS-T cancellation and P wave detection," in *Proc. Comput. Cardiol.*, Sep. 2012, pp. 37–40.

[28] W. Wenger and P. Kligfield, "Variability of precordial electrode placement during routine electrocardiography," *J. Electrocardiol.*, vol. 29, pp. 179–184, Jul. 1996.

[29] J. Garcia-Niebla, "Comparison of p-wave patterns derived from correct and incorrect placement of V1-V2 electrodes," *J. Cardiovasc. Nurs.*, vol. 24, pp. 156–161, Mar. 2009.

[30] R. Woolson, "Wilcoxon Signed-Rank Test," in *Wiley Encyclopedia Clinical Trials*, Hoboken, NJ, USA: Wiley 2008.

[31] G. Sanchez and M. De La Salud, "Activation patterns in atrial fibrillation: Contributions of body surface potential mapping," Ph.D. dissertation, Univ. Politècnica de València, Valencia, Spain, 2009.

[32] D. Giacopelli *et al.*, "Spatial pattern of P waves in paroxysmal atrial fibrillation patients in sinus rhythm and controls," *Pacing Clin. Electrophysiol.*, vol. 35, pp. 819–826, Jul. 2012.

[33] R. E. Mason and I. Likar, "A new system of multiple-lead exercise electrocardiography," *Amer. Heart J.*, vol. 71, pp. 196–205, Feb. 1966.

[34] B. J. Drew *et al.*, "Practice standards for electrocardiographic monitoring in hospital settings" *Circulation*, vol. 110, pp. 2721–2746, Oct. 2004.

Authors' photographs and biographies not available at the time of publication.